

The application of satellite data for detection and monitoring of methane emissions and the integration opportunities with weather and plant sensor data.

Ian Spence, Director for Datastore and Platforms, GHGSat Inc., UK

Darren Steele, Consultant, Stiperstone Analytics Ltd., UK

This paper introduces the use of satellites and aircraft sensors to observe and measure methane greenhouse gas emissions directly from industrial sites. Building upon an introduction to the methods used to detect greenhouse gas emission events, the following outputs from GHGSat satellite data are also described,

- surface reflectance imaging from source data
- derived geophysical variables and concentration maps
- model-based emission rate estimates and factors affecting confidence

Examples of observed methane emissions are included, together with examples of how GHGSat satellite sensors are able to detect emission rates of the order of 250 kg/hr and lower at a spatial resolution of approximately 25 metres. Applications of space data in Oil Sands, Mining, Shale Gas and Hydroelectric Power Generation, to monitor effective emission reductions, are referenced to demonstrate cross-industry use cases.

The paper also describes how the application of space observation data can help industrial facilities to decarbonize their activities and enhance environmental reporting with improved emissions monitoring coverage and leak risk assessment. Data-driven decision support in response to observed emission event response is explored by augmenting satellite data with integrated weather data streams and site-based, plant sensor data feeds. The paper concludes with examples of analytics that are applied to integrated data sets with prototypes for real-time methane plume characterisation and pre-event pattern searching.

1 Introduction

Methane emissions contribute to global warming, and it is also extremely flammable, colourless, odourless and tasteless (PHE, 2015). Therefore, methane presents several hazards across multiple industries and has led to many fatalities and lost time incidents at industrial plants. Methane readily forms explosive mixtures that can be ignited when mixed with air. With an ignition source, methane is explosive at concentrations between 50,000pm to 150,000ppm (Doss et al., 2021). Methane can also displace oxygen inside an enclosed space, leading to asphyxiation at 500,000ppm (Doss et al., 2021). The following incidents demonstrate the high potential safety and environmental risks from Methane,

- June 9, 2009, four workers were killed and sixty seven (67) others were injured in a natural gas explosion at the ConAgra Foods Slim JimTM processing facility in Garner, North Carolina. (CSB, 2009)
- February 7, 2010, six workers were killed and at least fifty (50) others were injured in a natural gas explosion at the Kleen Energy power plant under construction in Middletown, Connecticut. (CSB, 2010)
- February, 2018, The New York Times reported a gas-well accident at an Ohio fracking site and claimed that it resulted in one of the largest methane leaks ever recorded in the United States (Hiroko, 2019), a claim supported by satellite measurements of the incident (Pandey, 2019).
- September, 2021, The Chemical Engineer, reported high methane emissions from the coal-mining Boen Basin in Australia with an average methane release of 1.6 m t/y in 2019 and 2020, equivalent to 134m t/y of CO_2. (TCE, 2021)

The high potential catastrophic safety and environmental risks of methane are current and omnipresent. Therefore, monitoring, detection and mitigation of methane emissions and loss of containment requires increased research and development. This paper explores the use of satellite data to advance the measurement of atmospheric methane from space, with an exploration of how satellite data can be integrated with plant-based sensor data to help industrial facilities to respond to, and prevent, methane leaks.

2 Observing and measuring methane greenhouse gas emissions from space

Satellites offer unique benefits when used as observation platforms for monitoring human activities. Observations can be made at regular intervals at sites all around the world, even in remote locations, with the data from multiple occasions and between sites being directly comparable.

The orbital motion of a satellite is completely predictable, so overflights of a given site will occur at a known interval every few days. Regular satellite observations are a cost-effective way to quicky detect and quantify larger unplanned methane emissions, and complement the occasional site visits, aircraft surveys, or in situ sensors, where these are deployed. Particularly in more remote locations, the satellite option can represent a significant enhancement in the level of emissions monitoring.

Since the late 1990s over a dozen satellite missions have advanced the measurement of atmospheric methane from space (Jacob et al., 2016). They all do this by measuring methane’s absorption of specific wavelengths of infrared radiation. The earliest example is the Japanese IMG sensor launched in 1996 (Clerbaux et al., 2003) that measured the longer wavelengths of thermal infrared radiation emitted from the Earth's surface. Other sensors look in the short-wave infrared (SWIR) portion of reflected solar radiation, the first of these being the European SCIAMACHY instrument (Frankenberg et al., 2006) which operated from 2003 to 2012. More missions using these two sensing concepts have followed since (Jacob et al., 2016). One additional concept for future sensors is an active lidar or laser instrument (Kiemele et al., 2011) that would also operate in the SWIR region.

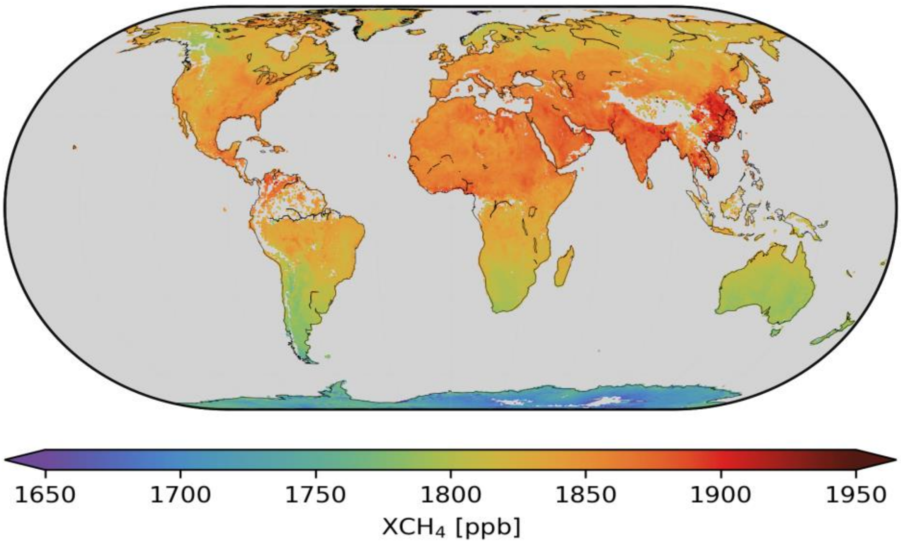

Figure 1. Global methane from TROPOMI sensor (Image: Copernicus/ESA/SRON, 2019)

The European Union's TROPOMI sensor began operations in 2017 and for the first time offers a daily global picture of atmospheric methane (Hu et al., 2018), albeit at a low spatial resolution of 7x5.5km. The TROPOMI sensor detects reflected SWIR radiation to give high accuracy data about overall concentrations of atmospheric methane (Figure 1). However, its use is limited in the direct monitoring of emissions or identification of sources since it is sensitive to only much larger emissions with rates of at least several tons per hour. By contrast, the launch in 2016 of the GHGSat-D "Claire" demonstrator satellite (Jervis et al., 2021) proved the feasibility of targeted satellite measurements at high resolution of smaller point-source methane emissions and justified the building of follow-on satellites with improved performance (Figure 2). In this case, the sensor can see individual methane plumes and enable their point of origin to be identified (Varon et al., 2019). Combining the measured local excess of methane with wind data allows the emission rate to be calculated (Varon et al., 2018).

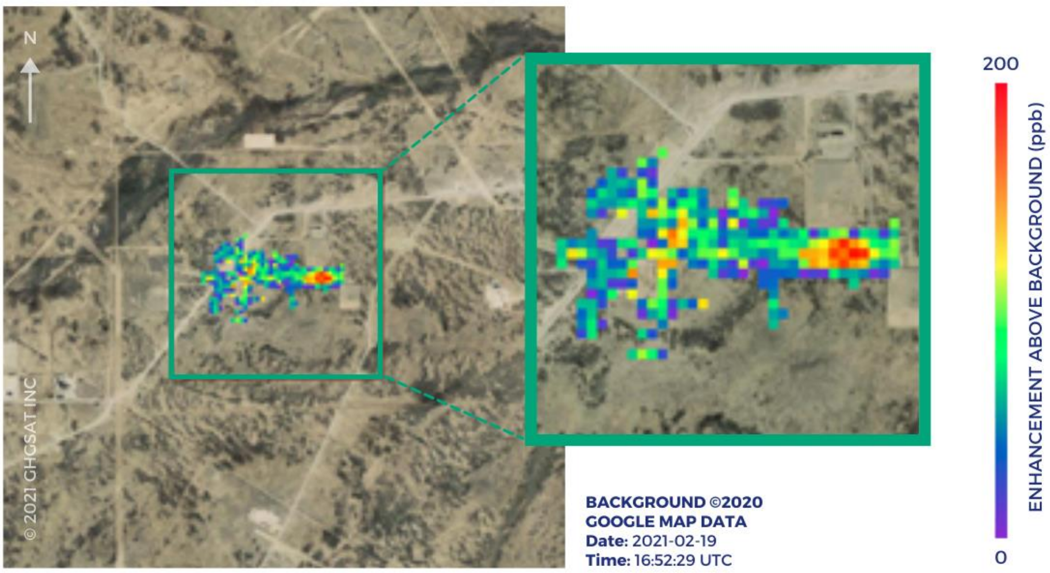

Figure 2. Methane emission observed in Permian Basin by GHGSat constellation satellite

GHGSat is the only commercial organisation operating satellites with high-resolution, high sensitivity methane sensors. The company's first two constellation satellites came online in September 2020 and January 2021 respectively. They enable GHGSat to offer monthly monitoring of customer assets worldwide and will be joined in 2022 by an additional three satellites. Further expansion of the constellation will continue in 2023 to a total of 10 orbiting sensors providing more capacity to monitor more sites, more frequently. The new GHGSat satellite sensors have 10x improved sensitivity to methane compared with the original patented technology from 2016 and are able to detect methane emissions with rates as low as 100kg/hr.

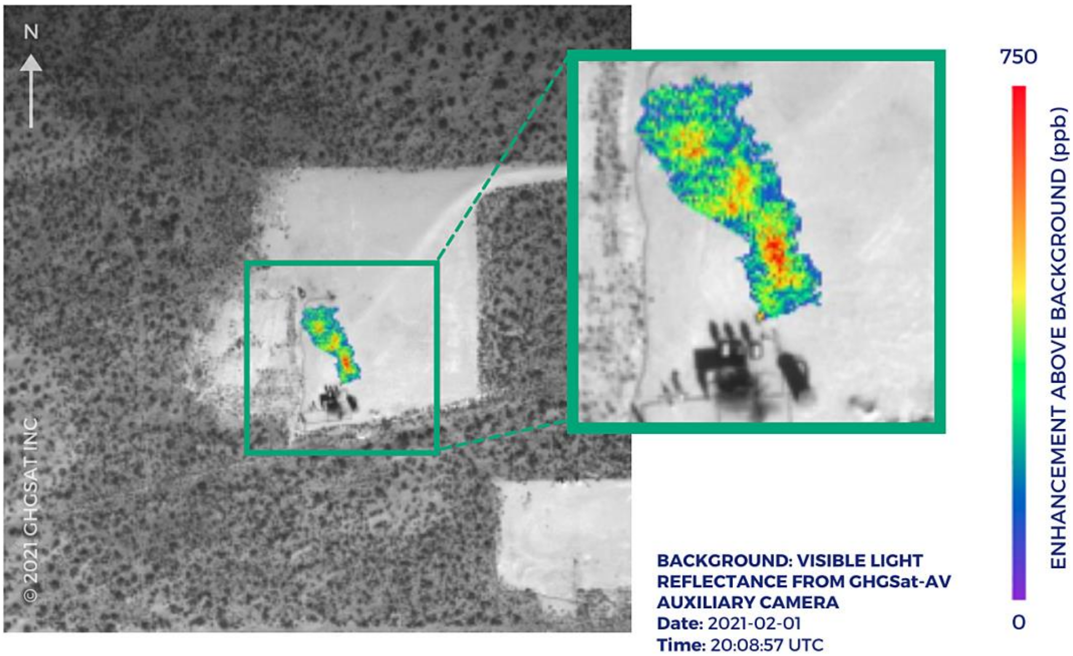

Figure 3. Methane emission observed in Permian Basin by GHGSat aircraft sensor

As a complement to GHGSat's own targeted satellites, there are several other satellites that regularly map the whole world and have been found to have sensitivity to at least larger methane emissions of a few tons or more per hour, despite not being designed for this purpose. GHGSat has published its peer-reviewed techniques to derive methane emissions from these public data (Varon et al., 2021) and operationally generates emissions notifications for sites all around the world. GHGSat has also developed a version of its sensor compatible with survey aircraft. The first of these sensors has been operational in North America since late 2019 and is able to detect smaller methane emissions of just 10kg/hr with a spatial resolution finer than 1 metre from 10,000 feet flying altitude (Figure 3). A second example of the GHGSat aircraft sensor will be operational before the end of 2021 and more are planned.

3 Integrating Satellite Observation Data for Analytics

The capability of satellites to detect and quantify emissions, and the overall accuracy of this data is influenced by many factors, including,

- Spatial Resolution (Level of detail of surface area coverage)
- Temporal Resolution (Frequency of observations from satellite passes)
- Wind Direction, speed & rotation
- Dispersion Characteristics
- Cloud Coverage

These factors impinge upon data reliability and confidence. Furthermore, the acquisition timestamp of satellite observation is not necessarily the start time of the emission event. Likewise, the last known positive observation does not represent the termination of the emission plume event.

Therefore, there is added value in cross referencing the satellite emissions observations with data gathered from plant and factory level sensors and instrumentation. The cross referencing of the disparate data sets is vital to improve the accuracy of the methane plume event, in terms of actual start date, actual end date, duration and quantity of methane released during each event.

The integration of the disparate data sets is performed using a commercial analytics software package from Seeq Corporation, Inc. The analytics software is applied to explore the following,

1. how disparate sets can be integrated to help improve the confidence and quantification of the methane plume event detection data
2. to develop a method for repeatable, automated cross referencing of satellite derived data streams with ground-based sensor data
3. to explore if an analytics platform can be used to recognise data patterns and plant anomalies leading up to a methane plume event and then search the data sets for other occurrences of the anomaly pattern
4. to develop a method to scan current plant data and identify emerging data patterns that match the known pre-event patterns, thereby providing potential for early warning and opportunity for plume event avoidance

To explore potential methods, the following simulated data sets are defined as inputs for the analytics platform,

- an emulated plant time-series data set containing process variables (Chen, 2019)
- a hypothetical sample of GHGsat observed data in comma separated variable format (csv) based upon GHGsat data set outputs in Figure 4
- weather data feed from National Oceanic and Atmospheric Administration (NOAA) National Weather Service

Figure 4. Example GHGSat Observation data set

Observation ID	File Basename	Country	Acquisition time [UTC]	WGS-84 Latitude [∞]	WGS-84 Longitude [∞]	UTM Easting [m]	UTM Northing [m]	UTM Zone	Q-IME [kg/hr]	Q-IME Error [%]	Source # Varon 2019	Event Varon 2019
1BEVxRS	GDSW1_SON1BEVxRS200717_CON1611280025_COLN01_TIFF	Canada	22/02/2018 18:10	53.911944	-117.2750095	481935	5973759	11 N	9100	100%+		
1D17F1K	GDSW1_SON1D17F1K200717_CON0018000445_COLN01_TIFF	Turkmenistan	19/06/2018 06:29	38.49391	54.19763	255596	4264340	40 N	11600	76%	1	a
1DwXF1K	GDSW1_SON1DwXF1K200717_CON0018000445_COLN01_TIFF	Turkmenistan	15/08/2018 06:29	38.49391	54.19763	255596	4264340	40 N	9900	69%	1	b
1ED4F1K	GDSW1_SON1ED4F1K200717_CON0018000445_COLN01_TIFF	Turkmenistan	03/09/2018 06:28	38.49391	54.19763	255596	4264340	40 N	43300	27%	1	c
1EXXk1K	GDSW1_SON1EXXk1K200717_CON0018000445_COLN01_TIFF	Turkmenistan	22/09/2018 06:27	38.49391	54.19763	255596	4264340	40 N	33400	48%	1	d
1FGXF1K	GDSW1_SON1FGXF1K200717_CON0018000445_COLN01_TIFF	Turkmenistan	08/11/2018 06:30	38.49391	54.19763	255596	4264340	40 N	30450	84%	1	e
1GIXk1K	GDSW1_SON1GIXk1K200717_CON0018000445_COLN01_TIFF	Turkmenistan	13/01/2019 06:26	38.49391	54.19763	255596	4264340	40 N	25450	62%	1	g
1GIXk1K	GDSW1_SON1GIXk1K200717_CON0018000445_COLN01_TIFF	Turkmenistan	13/01/2019 06:26	38.4992	54.2174	257339	4264874	40 N	33600	61%	2	g
2GWXk1K	GDSW1_SON2GWXk1K200717_CON0018000445_COLN01_TIFF	Turkmenistan	27/01/2019 06:27	38.49391	54.19763	255596	4264340	40 N	37850	48%	1	f
2GWXk1K	GDSW1_SON2GWXk1K200717_CON0018000445_COLN01_TIFF	Turkmenistan	27/01/2019 06:27	38.55947	54.20253	256245	4271603	40 N	2700	67%	3	h
1Dz0Xvv	GDSW1_SON1Dz0Xvv200717_CON0018000483_COLN01_TIFF	USA	17/08/2018 16:53	31.687004	-103.7251805	620825	3506449	13 N	1750	66%		

Q: Source Rate
IME: Integrated Mass Enhancement

With the observation data set, an acquisition timestamp is provided for each observation, and each of the snapshot observations provides an estimated mass flow rate of methane at the timestamp, together with a location and estimated error. When importing this data set into the analytics system, the derived mass flow rate of methane is expressed a step data point with an assumption that the methane flow rate is constant until the next observation that records a different mass flow rate. Figure 5 displays the step type trend resulting from the import of the data set. The analysis platform is then used to define a condition that will scan the entire data set and generate capsule events that represents the duration of each methane plume event from the connected data set.

Figure 5. Satellite derived methane plume event observation data with conditional logic to indicate plume duration

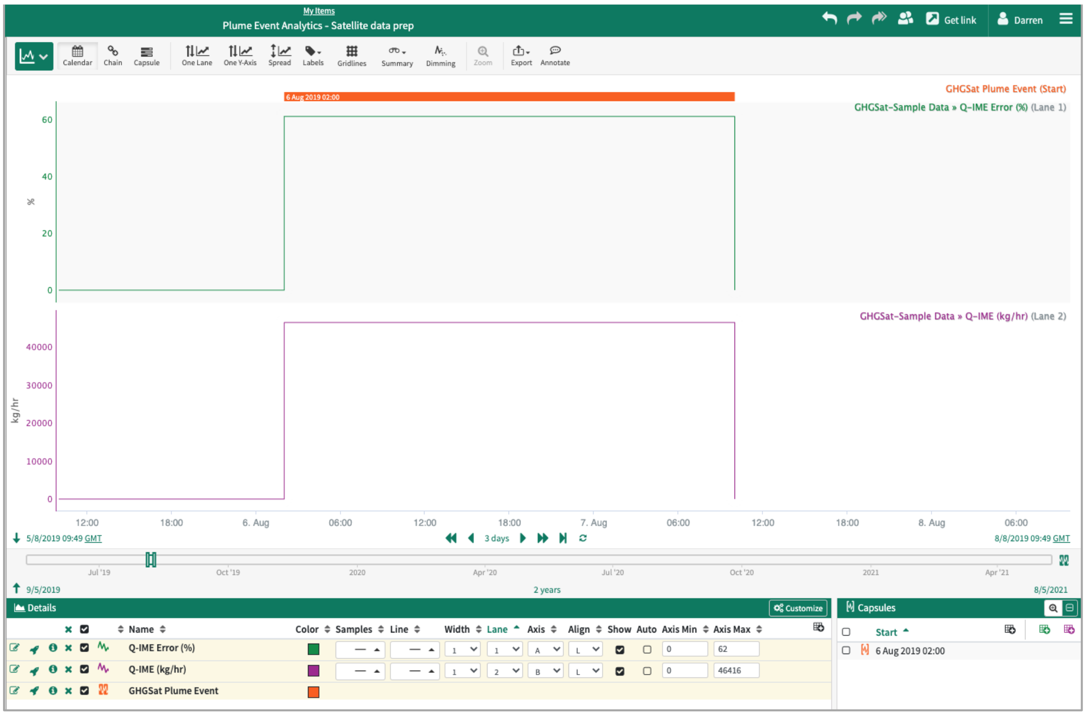

Figure 6 then displays plant sensor data trend lines for a period of time around the satellite derived methane plume event. The red event capsule signifies the Satellite observed plume event. Conditional logic can then be applied to identify corresponding step changes in associated plant sensor data. A second series of event capsules (blue bar) are then derived providing more accurate plume event durations and bounding timestamps.

Figure 6. Cross referencing simulated satellite observed Methane plume data with simulated plant data and determination of more accurate plume event properties.

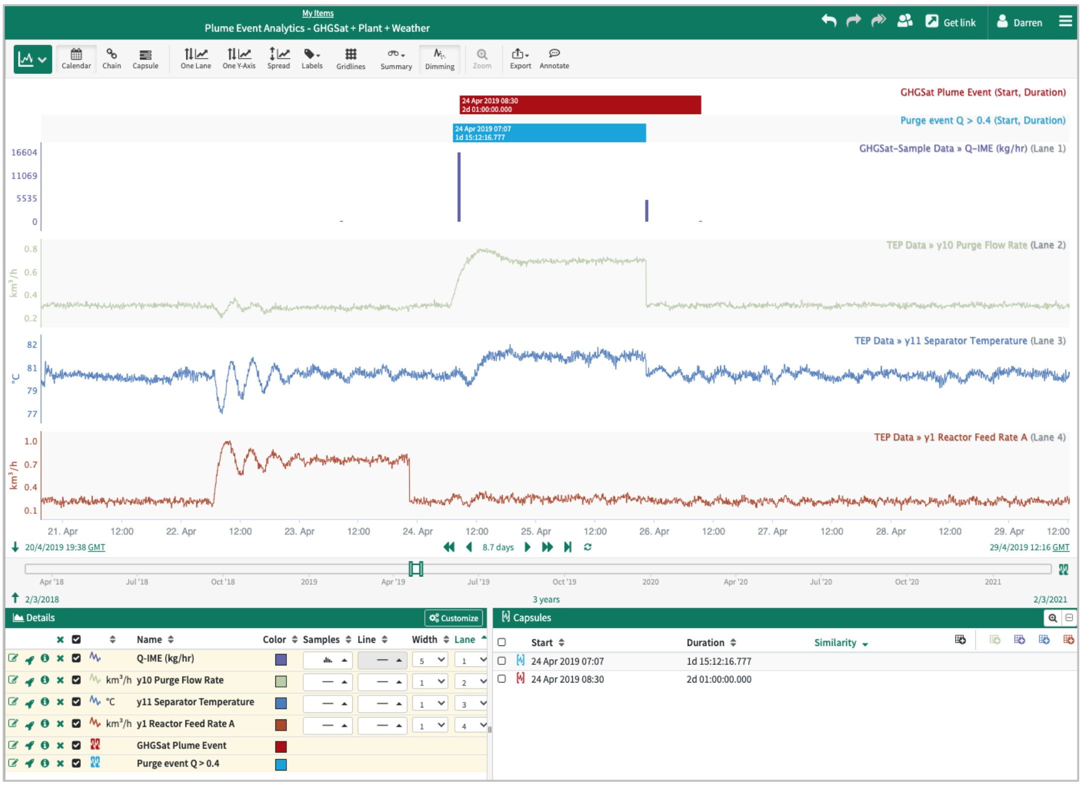

This visual analysis facilities identification of plant disturbances prior to methane plume event capsules and these disturbance patterns are then used to check for emerging patterns that match the known disturbance pattern.

The next step in the analysis is to derive the actual mass of methane released using the improved event property data. The duration of the event and the volumetric flowrate is used to convert from the volumetric flowrate to the mass and the output is stored in a soft sensor displayed in Figure 7

Figure 7. Automated calculation of methane mass for each plume event and display in a soft sensor

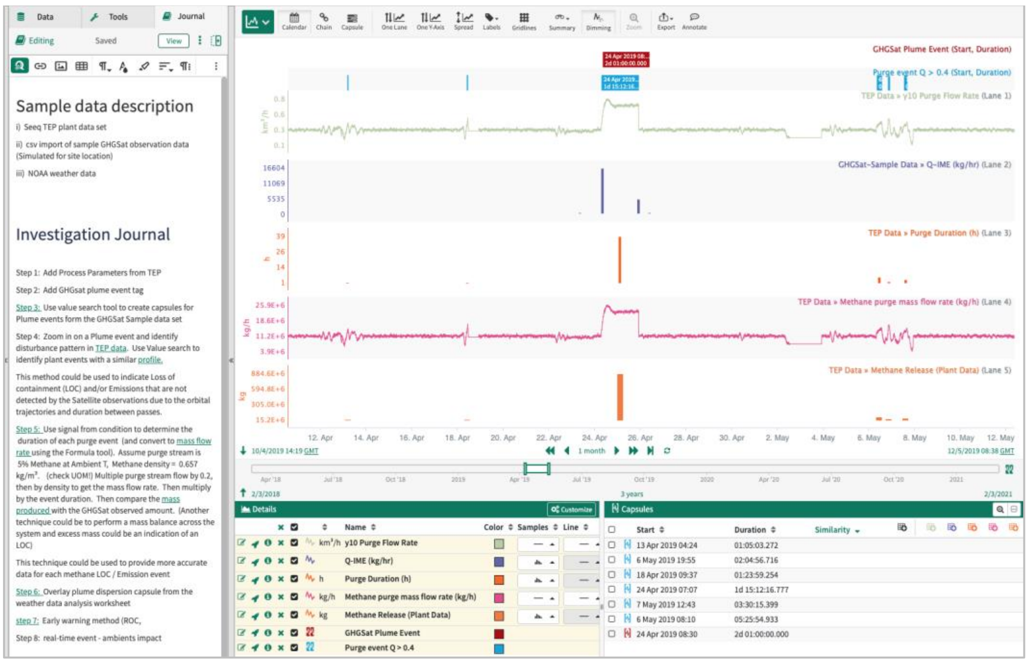

The conditional event detection rule that is used to determine the more accurate methane plume events and event properties is then applied to the current and historical plant data feed to identify matching periods of operation that could indicate repeat occurrences of the methane plumes. These events are highlighted with the blue event capsules in figure 8. There are several methods available for the detection rule, including a value search method based on one or more process variables exceeding a defined threshold. Another method that can be deployed is to select of a pattern from the trend and to use the application to search for patterns that are similar, with matching patterns being indicated with new capsules.

Figure 8. Applying the conditional event detection rule to identify potential repeat occurrences in the historical plant data feed

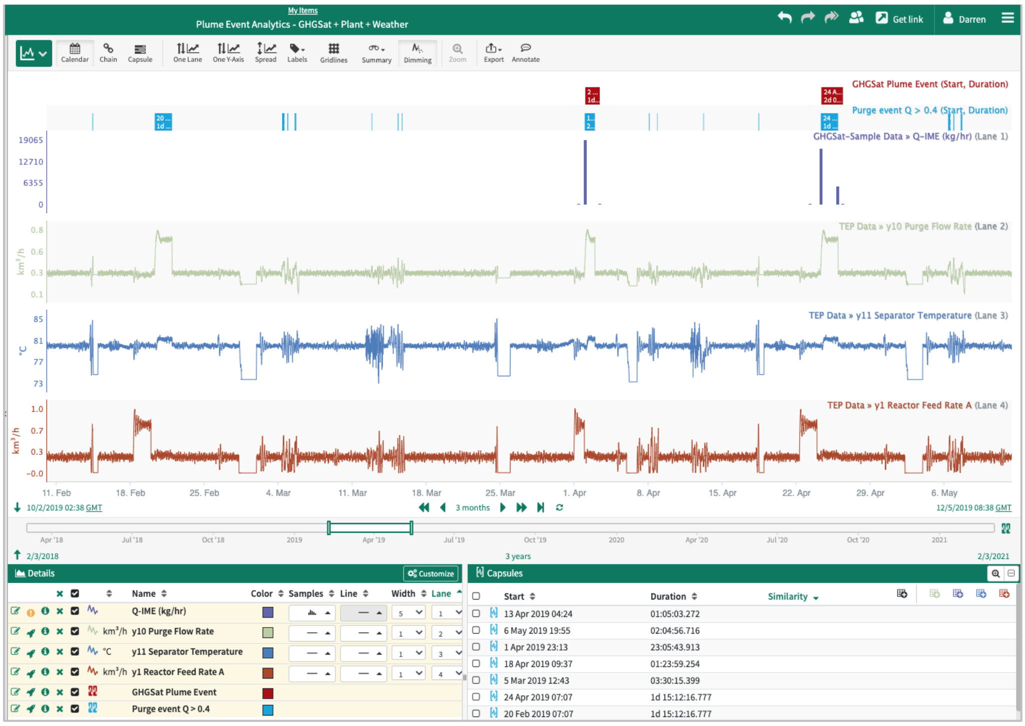

This prototype presented in this paper further demonstrates a method for integrating data sets related to methane plume events and subsequent analysis of the data sets to derive further insights that could aid in improving accuracy of plume event properties and mitigation from earlier warning of emerging events.

A NOAA Weather data feed (Chen, 2019) was also integrated into the analytics system creating scope to determine the characteristics of the methane plumes. Plumes can be grouped into stable, neutral and unstable plume types and the plume behaviour is a function of lapse rate, temperature, dew point temperature, wind speed, wind direction (Rodos, Thykier et al, 1999). Temperature readings must be sampled at multiple heights and cross referenced with the wind speed to determine plume behaviour. This would require multiple land-based sensors at different heights local to the industrial facility as the weather service station data is typically sampled at an international standard of 10 metres from ground level with questionable proximity to the facility. However, the purpose of this paper is to scope the integration opportunities and the simplified prototype model displayed in figure 9 displays NOAA weather data integrated with simulated pant data. The analysis also shows the weather data and plant data can be used to estimate plume behaviour in case of an emission event. Unstable plume conditions are highlighted using blue event capsules, green capsules indicate stable plume dispersion, and purple capsules indicate conditions for neutral plume dispersion behaviour.

Figure 9. Integrating Weather Data for real-time determination of Plume Characteristics

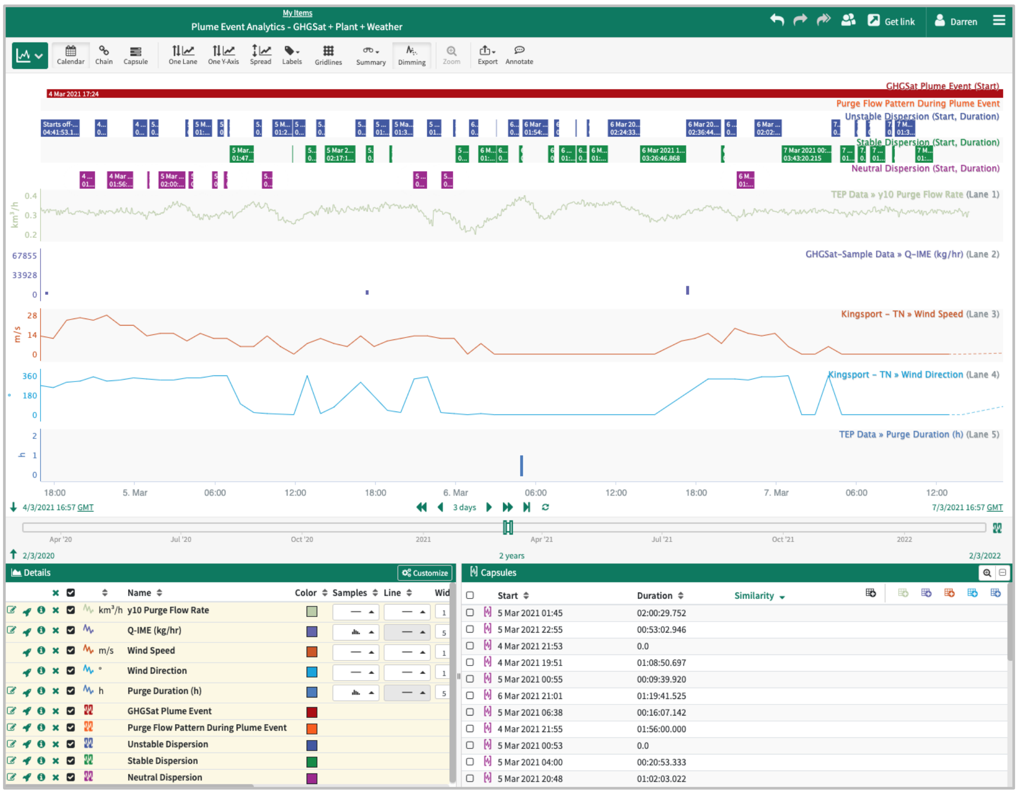

Suggestions for Future Work

The prototype for cross referencing satellite observed data with plant-based data should be validated using known observations and related methane plume event data from a plant operator. This will facilitate the validation of plume event detection, the methods provided to analyse the plant operation leading up to the event, the subsequent root-cause identification, and the potential for earlier warning of emerging methane leak events.

Potentially, a library of plant data failure patterns can be developed and shared between similar plants and operations to aid preventive mitigation of methane plume events.

The data integration aspect of this paper focuses on integration with factory and plant sensors and instrumentation, however, the majority of emissions in 2018 were attributed to agricultural processes and waste management activities (Brown, Hayward et al, 2021). Therefore, integration with land based sensors from agricultural and waste management sites should also be explored.

This paper focuses on methane plume detection, however, there are other harmful gases with extreme global warming potential that should be considered for research and development for measurement from Satellites e.g. ammonia, nitrogen dioxide detection are also important, and especially fluorinated gas leak detection from industrial scale refrigeration and air conditioning processes.

Spatial and temporal coverage improvements and the advent of miniaturised satellites and geostationary satellites could eventually lead to near real time coverage that could provide improvements to emergency response and earlier curtailment of leaks.

Real-time plume and dispersion characterisation, triggered by near real time event detections from greenhouse gas satellite observation data providers should also be explored to enhance the prototype model described in this paper.

References

Doss, Howard J., McLeod, William, Person, Howard L. (Retrieved 2021, September 1) Beware of Manure Pit Hazards. Michigan State University Extension, National Ag Safety Database, https://nasdonline.org/1292/d001097/beware-of-manure-pit-hazards.html

U.S. Chemical Safety and Hazard Investigation Board (CSB) ,September 2009 , Dangers of Purging Gas Piping into Buildings, Safety Bulletin , No. 2009-12-I-NC , Retrieved on 1st September from https://www.csb.gov/conagra-natural-gas-explosion-and-ammonia-release/

U.S. Chemical Safety and Hazard Investigation Board (CSB) ,June 2010, Kleen Energy Natural Gas Explosion Final Report. Retrieved on 1st September from https://www.csb.gov/kleen-energy-natural-gas-explosion/

Public Health England (PHE) 2015, Methane Incident Management, PHE publications gateway number: 2014790

Brown, A., Hayward, T., Timmis, R, Wade, K, Pope R, Trent, T., Boesch H, Guillo, R.B., 2021, Satellite measurements of air quality and greenhouse gases: : application to regulatory activities, Chief Scientist's Group report, Environment Agency, Version: SC200001/R.

Clerbaux, C., Hadji-Lazaro, J., Turquety, S., Mégie, G., and Coheur, P.-F.: Trace gas measurements from infrared satellite for chemistry and climate applications, Atmos. Chem. Phys., 3, 1495– 1508, doi:10.5194/acp-3-1495-2003, 2003.

Frankenberg, C., Meirink, J. F., Bergamaschi, P., Goede, A. P. H., Heimann, M., Körner, S., Platt, U., van Weele, M., and Wagner, T.: Satellite chartography of atmospheric methane from SCIAMACHY on board ENVISAT: Analysis of the years 2003 and 2004, J. Geophys. Res., 111, D07303, doi:10.1029/2005JD006235, 2006.

Hu, H., Landgraf, J., Detmers, R., Borsdorff, T., aan de Brugh, J., Aben, I., et al.: Toward global mapping of methane with TROPOMI: First results and intersatellite comparison to GOSAT. *Geophysical Research Letters*, *45*, 3682–3689. https://doi.org/10.1002/ 2018GL077259, 2018.

Jacob, D. J., Turner, A. J., Maasakkers, J. D., Sheng, J., Sun, K., Liu, X., Chance, K., Aben, I., McKeever, J., and Frankenberg, C.: Satellite observations of atmospheric methane and their value for quantifying methane emissions, Atmos. Chem. Phys., 16, 14371–14396, https://doi.org/10.5194/acp-16-14371-2016, 2016.

Jervis, D., McKeever, J., Durak, B.O.A., Sloan, J.J., Gains, D., Varon, D.J., Ramier, A., Strupler, M., and Tarrant, E.: The GHGSat-D imaging spectrometer. Atmos. Meas. Tech., 14, 2127–2140, 2021 https://doi.org/10.5194/amt-14-2127-2021, 2021.

Kiemle, C., Quatrevalet, M., Ehret, G., Amediek, A., Fix, A., and Wirth, M.: Sensitivity studies for a space-based methane lidar mission, Atmos. Meas. Tech., 4, 2195–2211, doi:10.5194/amt-4- 2195-2011, 2011.

Pandey, S., Gautam, R., Houweling, S., van der Gon, H. D., Sadavarte, P., Borsdorff, T., et al. (2019). Satellite observations reveal extreme methane leakage from a natural gas well blowout. Proceedings of the National Academy of Sciences, 116, 26,376–26,381 https://doi.org/10.1073/pnas.1908712116, (201908712), (2019).

Rodos, & Thykier-Nielsen, S & Deme, Sandor & Mikkelsen, Torben. (1999). Description of the atmospheric dispersion module RIMPUFF.

Varon, D. J., Jacob, D. J., McKeever, J., Jervis, D., Durak, B. O. A., Xia, Y., and Huang, Y.: Quantifying methane point sources from fine-scale satellite observations of atmo- spheric methane plumes, Atmos. Meas. Tech., 11, 5673–5686, https://doi.org/10.5194/amt-11-5673-2018, 2018.

Varon, D. J., McKeever, J., Jervis, D., Maasakkers, J. D., Pandey, S., Houweling, S., Aben, I., Scarpelli, T., and Jacob, D. J.: Satellite discovery of anomalously large methane point sources from oil/gas production, Geophys. Res. Lett., 46, 13507–13516, 2019.

Varon, D. J., Jervis, D., McKeever, J., Spence, I., Gains, D., and Jacob, D. J.: High-frequency monitoring of anomalous methane point sources with multispectral Sentinel-2 satellite observations, Atmos. Meas. Tech., 14, 2771–2785, https://doi.org/10.5194/amt-14-2771-2021, 2021.

The Chemical Engineer (TCE), High Methane Emissions from Australia Coal Region, September 2021, Issue 963

Chen, X., (2019) "Tennessee Eastman simulation dataset", IEEE Dataport, taken from https://ieee-dataport.org/documents/tennessee-eastman-simulation-dataset under Creative Commons Attribution